Proceeding of the IEEE
International Conference on Robotics and Biomimetics
Dali, China, December 2019

A Robotic Charging Scheme for Electric Vehicles Based on Monocular Vision and Force Perception

Xincan Lv, Guangzeng Chen, Haopeng Hu and Yunjiang Lou

***Abstract*— Electric Vehicles are rapidly gaining popularity worldwide. The main two problems limiting their use are the short driving distance and inconvenient charging process. In this paper, we propose a technical scheme for opening the cover and inserting the plug into the charging port autonomously based on monocular vision guidance technology and force sensing technology. The whole system consists of a monocular camera, an UR5 robot with the plug mounted at the end and a charging port. The process firstly obtains the pixel coordinates of the target, and then calculates the spatial position of the target, thereby guiding the robot arm to complete the operation of opening the cover. Then the SVM algorithm is applied to analyze the force/torque data during the plug-in-hole process. The plug is inserted into the hole according to the data analysis result. Finally, the feasibility of the proposed scheme is demonstrated in a series of successful experiments.**

***Index Terms*— Monocular vision, Eye-in-hand calibration, Robotic vision guidance technology, Force perception technology, SVM**

I. Introduction

With the gradual promotion and use of electric vehicles, its supporting infrastructure needs to be vigorously developed. However, a new problem being faced by electric vehicles is having an accessible, fast and convenient battery charging, especially when travelling longer distance. A solution to this problem would be a robotic charging system combined with automated car parking.

Robotic charging solutions have been extensively studied both in academic and industrial environments. Tesla, Volkswagen and many other companies have all proposed their own concept of automatic charging [1]. However, the specific technical details have not been revealed. The process of robotic charging is a practical application scenario of the robotic peg-in-hole technology. Both vision and force control techniques are used for robotic peg-in-hole operations [2]. 2D cameras are widely used for coarse localization by extracting the boundaries of holes from images [3]. Chang et al. [4] and Huang et al [5] proposed position-based visual servo systems with fast convergence guarantees based on the image calibration method and limited calibration. In contrast, stereo cameras (Kinect) have been applied to capture the 3D point data to estimate the accurate 3D poses of mating parts [6]. The force control strategy has been extensively researched and applied in various fields [2]. Inoue et al. proposed a force-based assembly control strategies [7]. However, their approach has high requirements for the hardware structure. Wang, et al presented a novel contact force/torque prediction and analysis model to solve the large length-diameter ratio peg-in-hole assembly problem [8]. In addition, instead of determining the contact state by calculating the similarity, classification algorithms, such as support vector machine (SVM), have been applied to determine the contact state [9].

Although these methods above can solve peg-in-hole problems in some scenarios. It is difficult to peg in hole assembly in actual scene. Moreover, in the process of automatic charging of electric vehicles, the cover opening operation plays a crucial role in the entire process. But the cover opening operation has been rarely mentioned.

In this paper, we propose a technical scheme for the scene of robotic charging of electric vehicles. We abstract the robotic charging process into two parts: the cover-opening operation and the plug-in-hole operation. We firstly performed an offline eye-in-hand calibration to obtain the relative position of the camera and the end of the robotic arm. We establish a coordinate system for the feature area, and then use perspective-n-point (PnP) algorithm to obtain the relative position between the camera and the tag, whose position relative to the cover is fixed. According to the relative position information, the UR5 robot arm with the plug mounted at the end reaches the relative position set before. Then the end of the arm completes the opening operation by moving in accordance with the L-shaped path. After that, we design a plug-in-hole scheme based on the SVM classifier algorithm. According to the scheme, the robot arm is guided to adjust the end position in real time, and the plug-in-hole operation is completed finally.

The rest of the paper is organized as follows. The structure of the system is described in Section II. Section III explains the details of our proposed scheme, including the process of the cover opening operation and the specific steps of the plug-in-hole operation. Section IV shows the experiment results and proves that the scheme is effective. In Section V, we conclude the paper with some suggestions for future work.

This work was supported partially by the NSFC-Shenzhen Robotics Basic Research Center Program (No. U1713202) and partially by the Shezhen Science and Technology Program (No. JCYJ20160429115309834 and No.JCYJ20180508152226630).

Lv, Chen, Hu and Lou (the corresponding author) are with the School of Mechatronics Engineering and Automation, Harbin Institute of Technology Shenzhen, HIT Campus, University Town of Shenzhen, Xili, Nanshan, Shenzhen, China. (louyj@hit.edu.cn)

978-1-7281-6321-5/19//$31.00 ©2019 IEEE

II. Operation Process

As shown in Fig. 1(a), our actuator is a UR5 robot arm with a charging plug, a force/torque sensor and a 2D camera mounted ar the end. Fig. 1(b) shows the charging port with the white square label when the cover is closed. When the cover is open, the hole in Fig. 1(c) will be exposed. The goal of our entire technical scheme is to guide the robot to complete the operation of opening the cover in Fig. 1(b), and then peg the charging plug into the hole of the charging port in Fig. 1(c). These operations play an essential role in the automatic charging process of the electric vehicles.

(a) (b) (c)

Fig. 1. Eye-in-hand Manipulator: (a) The robot arm with the camera and the plug mounted at the end; (b) The charging port with the cover closed; (c) The charging port with the cover open

The cover opening operation process is divided into the following three steps. First, the robot moves the connection plug to the approach position, which is about 0.2 meter away from the charging port cover. In the second step, the robot moves in an L-shaped path from the approach position in order to complete the opening operation. After that, the robot moves to the approximate alignment of the socket. Finally, the end position is adjusted in real time according to the force/torque data until the plug-in-hole operation is completed. The schematic diagram of the whole process is shown in Fig. 2. In addition, the structure of the end has a certain flexibility. After opening the cover, the structure of the charging port is shown in Fig. 3. The structure has a guiding effect on the end of the arm. These factors play a beneficial role in the plug-in-hole operation.

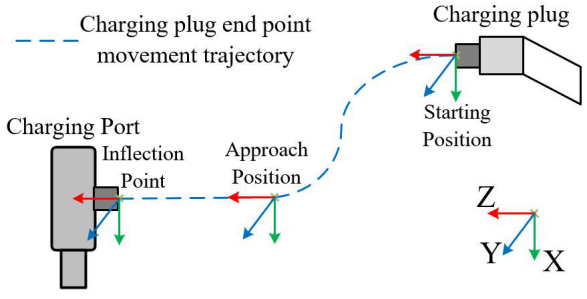

Fig. 2. Three steps in the over opening operation

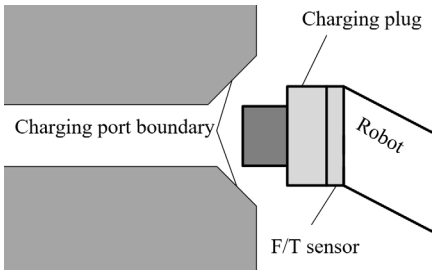

Fig. 3. The hole structure diagram of the charging port

III. Method

A. Overview

Our purpose is to achieve cover opening operation and plug-in-hole operation. A monocular camera is used to detect, localize the target and guide the robot to move correspondingly. Except the monocular camera, we do not use any other extra vision sensors, such as depth cameras. But to ensure the safety of the equipment, we mount a force/torque sensor at the end of the arm. Our approach is to mimic human manipulation as much as possible. We human beings also use our eyes to detect and locate the charging port. Then move the charging plug to the corresponding position, and pegging the plug into the charging port while adjusting the plug. In this paper, the camera is the eye of the robot, and the end with the forque/torque sensor is equivalent to the wrist of the robot. Moreover, SURF algorithm is used for initial localizing. Then our method obtains the corresponding depth information by establishing the size correspondence of the target area, and guides the robot arm to complete the cover opening operation and plug-in-hole operation. The architecture of the robotic charging system is as shown in Fig. 4.

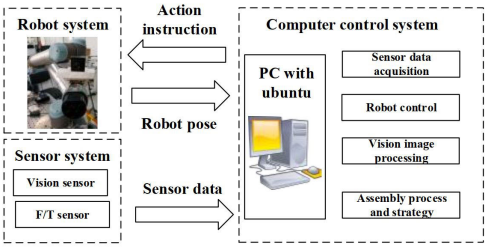

Fig. 4. The architecture of the robotic charging system

B. Relative Pose Calculation

Our method first obtains the pixel position of the target area. Then we establish a spatial Cartesian coordinate system in the target area so that we can obtain the spatial three-dimensional position of the tag relative to the camera through the perspective-n-point (PnP) algorithm. Through the eye-in-hand calibration, the spatial position of the tag relative to the

end of the robot can be obtained finally.

A majority of the car charging ports are manufactured from texture-less black plastic material, making it difficult to obtain good features in the camera image, especially for monocular vision. As shown in Fig. 1(b), our method uses the tag on the cover as the detection object. In order to match the camera view and the template which is manually captured at the specific position, a scale-invariant and rotation-invariant feature detector and descriptor is required. The process needs to detect enough interest points that ensures the robustness of the matching. Speeded Up Robust Features(SURF) [10] algorithm is applied for feature detection and matching in our work. The feature is obtained by relying on integral images for image convolutions and using a Hessian matrix-based measure for the detector. Besides, the features are both scale-invariant and rotation-variant, which is essential for our detection. The template picture is shown in Figure. 5, and the detection effect is as shown in Fig. 6. After the above process, we will get the pixel coordinates of the four corner points of the target area.

Fig. 5. The template image

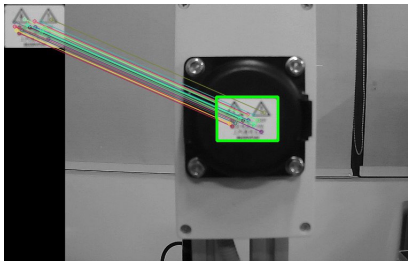

Fig. 6. Template image matching effect

As shown in Fig. 7, we can get the pixel coordinates of the four corner points. And then we take the A point in the upper left corner of the figure as the origin, the direction of the ray AB as the positive direction of the X-axis, and the direction of the ray AC as the positive direction of the Y-axis so that we can establish A-xyz space rectangular coordinate system. The spatial coordinates of points A,B,C,D in the A-xyz space coordinate system are obtained by actual measurement, which are A(0,0,0), B(34,0,0), C(34,24,0) and D(0,24,0). The unit is millimeters.

After obtaining the actual spatial 3D coordinate values and pixel 2D coordinate of the A, B, C, and D 4 points, we use the perspective-n-point (PnP) algorithm to perform 3D pose estimation between the tag of the charging port and the camera [11] [12]. Our method finally obtains the

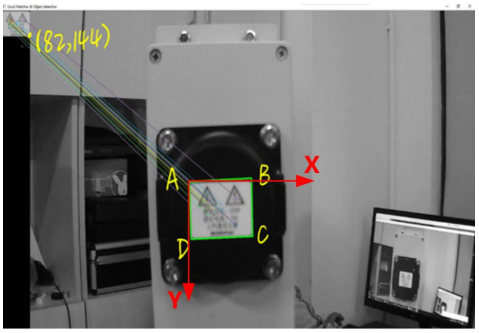

Fig. 7. Schematic diagram of space rectangular coordinate system

spatial position of the tag to the end of the manipulator by performing a off-line eye-in-hand method. There are several PnP algorithms such as EPnP, DLT and UPnP. The EPnP algorithm is used in our method. The EPnP algorithm is based on the P3P algorithm, The schematic diagram of the P3P algorithm is as shown in Fig. 8.

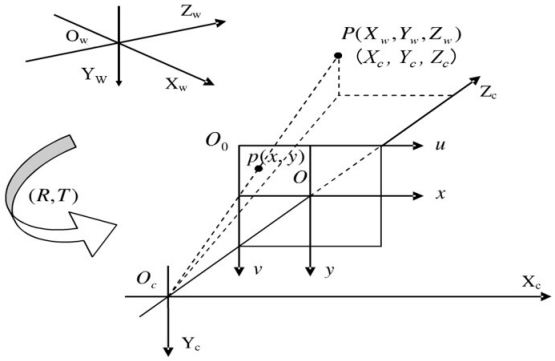

Fig. 8. The schematic diagram of P3P algorithm

As shown in the Fig. 8, the space coordinates of the P point in the world coordinate system, called A-xyz coordinate system, are $P_w(X_w,Y_w,Z_w)$, and the coordinates of the P point in the camera coordinate system are $P_c(X_c,Y_c,Z_c)$. (x,y) is the pixel coordinates of the P point in the picture. According to the geometric relationship, the following equations can be obtained.

$$\begin{cases} X_c = \frac{\frac{x}{f_x} \times OP}{\sqrt{(\frac{x}{f_x})^2+(\frac{y}{f_y})^2+1}} \\ Y_c = \frac{\frac{y}{f_y} \times OP}{\sqrt{(\frac{x}{f_x})^2+(\frac{y}{f_y})^2+1}} \\ Z_c = \frac{1 \times OP}{\sqrt{(\frac{x}{f_x})^2+(\frac{y}{f_y})^2+1}} \end{cases} \quad (1)$$

In this way, if we obtain the values of the four different spatial points $P_c^1, P_c^2, P_c^3, P_w^1, P_w^2, P_w^3$,, we will be able to find the transformation relationship matrix between the world coordinate system and the camera coordinate system. In our method, according to the actual space coordinates and pixel

coordinate values of 4 points we have obtained, we can calculate the relative position of the point A and the camera. The spatial coordinates of 4 points set in our method is shown in (2), which describes the physical coordinates of the four points A, B, C and D. The unit is mm. (3) shows the pixel coordinate result, and the unit is pixel. $[R, T]$ conversion matrix calculated are shown in the equation (4), where R represents the rotation vector between the camera and the arm end, and T represents the translation relationship. The unit of the values in T is mm.

$$A[0,0,0], B[34,0,0], C[34,24,0], D[0,24,0] \tag{2}$$

$$A[644,543], B[896,532], C[901,717], D[651,726] \tag{3}$$

$$\begin{bmatrix} R \\ T \end{bmatrix} = \begin{bmatrix} 0.21007382 & 0.13204134 & 3.0853392 \\ -18.12608231 & 29.11586704 & 267.60567687 \end{bmatrix} \tag{4}$$

C. Eye-in-Hand Calibration

After obtaining the position of the target tag relative to the camera, we need to know the position of the tag relative to the end of the manipulator. Our method implements it with an off-line Eye-in-hand calibration. Our method refers to the calibration method described in Tsai's method [11]. Our method fixes the calibration chessboard relative to the robot base. The end pose of the manipulator is read by the program from the UR5 robot control cabinet. The position of the calibration chessboard relative to the camera can be obtained from the captured image by means of the MATLAB calibration toolbox. The schematic diagram of the eye-in-hand calibration system is shown in the Fig. 9.

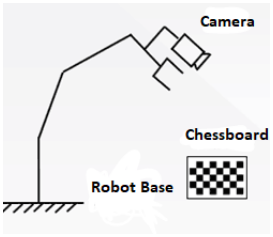

Fig. 9. Eye in hand system

$$^{R}_{E1}T\,^{E1}_{C1}T\,^{C1}_{O}T = {}^{R}_{E2}T\,^{E2}_{C2}T\,^{C2}_{O}T \tag{5}$$

$$^{R}_{E2}T^{-1}\,^{R}_{E1}T\,^{E1}_{C1}T = {}^{E2}_{C2}T\,^{C2}_{O}T\,^{C1}_{O}T^{-1} \tag{6}$$

Our calibration principle is illustrated in the equations (5) and (6). In the equations, $^{R}_{E}T$ represents the transition matrix of the end of the manipulator to the robot base. $^{E}_{C}T$ represents the transition matrix of the camera to the end. $^{C}_{O}T$ represents the transition matrix of the object to the camera. $^{R}_{E}T$ can be read from the controller by the program, and $^{C}_{O}T$ is calculated by the PnP algorithm of the previous part.

The specific solution process is solved here by using the method mentioned by Tsai in [11]. Our method took pictures and operated them when the end of the manipulator was at 20 different positions. The final solution results are shown in (7). After comparison with the actual structure of the end, our calibration results can meet our requirements.

$$res = \begin{bmatrix} -0.99464 & -0.06038 & -0.08394 & 0.04486 \\ 0.06751 & -0.99411 & -0.08474 & 0.09152 \\ -0.07833 & -0.08995 & 0.99286 & 0.16993 \\ 0 & 0 & 0 & 1 \end{bmatrix} \tag{7}$$

D. Plug-in-hole strategy

We assume that the end of the manipulator with the plug reaches the approach position after the above steps, and it is basically necessary to ensure that the plug and the port are already in a straight line. Then we control the end of the robot to move along the line until it touches the cover of the charging port. And then the robot moves right to open the cover. Combined with the output values of the PnP algorithm, our method calculates the ready insertion position and guides the robot to be ready for peg-in-hole operation. The schematic diagram of the movement of the end of the robot before opening the cover is shown in Fig. 2.

After the opening operation is completed, the robot moves the plug to be ready for plug-in-hole operation. Next, this section describes how to move the plug in conjunction with the real-time force/torque sensor data. The force/torque data we obtained can be expressed as $FM = [Fx, Fy, Fz, Mx, My, Mz]$, where F and M are the force and moment obtained from the force/torque sensor; the subscript x, y, z denotes the axis. As shown in Fig. 1 (c), the port hole is deep and the internal surface of the hole is complicated, which results that the force/torque data is nonlinear in the actual electric vehicles charging process.

As shown in Fig. 10, we collected the changes of Fx, Fy, Mx and My data in successful and unsuccessful plug-in-hole operation. It can be seen from Fig. 10(a) and Fig. 10(b) that in the case of successful insertion, the Fx and Fy values are distributed in the range of ($\pm$10 N)×($\pm$10 N), and the Mx and My values are distributed in the range of ($\pm$2 N·m)×($\pm$2 N·m). In addition, we can not determine whether to proceed with advancement only based on the values of $Fxy = \sqrt{(Fx)^2 + (Fy)^2}$ or $Mxy = \sqrt{(Mx)^2 + (My)^2}$. Therefore, we combined Fx, Fy, Mx, My in the force/torque data processing. First, the force/torque data is normalized as according to equation (8) and then used as a classifier input. The data after normalization is shown in Fig. 10(c) and (d). All normalized data is distributed in the range of $\pm 1 \times 1$.

$$X = ((\frac{F_x}{\max|F_x|})^2 + (\frac{F_y}{\max|F_y|})^2, (\frac{M_x}{\max|M_x|})^2 + (\frac{M_y}{\max|M_y|})^2) \tag{8}$$

Based on the approximately 200 sets of data we collected,

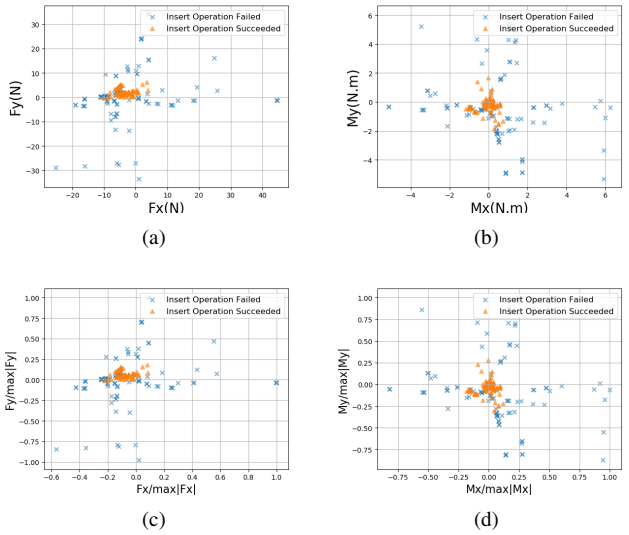

Fig. 10. Force data collected:(a) Fx and Fy numerical distribution map; (b) Mx and My numerical distribution map; (c) Normalized Fx and Fy numerical distribution map; (d) Normalized Mx and My numerical distribution map

we design a classifier based on the support vector machines (SVM) algorithm. We use X in (8) as the input to the classifier. Our classifier calculation formula is as shown in equation (9) and equation (10), where X refers to the input, V is the support vector we found from the data set, σ is 1, and e is natural base. The parameters w, b, and V can be trained by the training data set.

$$y = \text{sign}(w \times K(x) + b) \tag{9}$$

$$K(x) = e^{-\frac{||V-X||}{2\sigma^2}} \tag{10}$$

In the process of the actual experiments, the force/torque data is obtained in real time. If the classifier output is 1, it is judged that the advancement can be continued. Otherwise, the robot moves up, move down, move left or move right according to the magnitude of Fx and Fy. It is emphasized here that because the end of the robot is flexible, Mx and My will change with Fx and Fy simultaneously during the movement up, down, left and right, which is similar to the manual process. Therefore, we are currently using the four adjustment actions of up, down, left and right during the process of plug-in-hole operation. The magnitude of these four adjustment actions is the minimum distance that the robot can achieve during the plug-in-hole process. The adjustment strategy for the plug-in-hole process is as shown in Fig. 11. The process of the plug-in-hole operation starts from the contact of the plug with the charing port and continues until the z-coordinate of the end of the robot reaches the preset coordinate value.

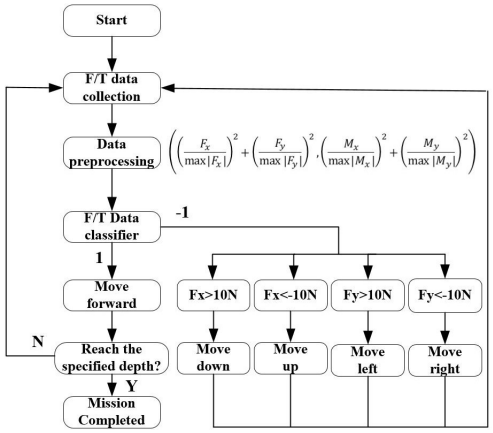

Fig. 11. Force control strategy

IV. Experiments and Results

To demonstrate the performance of the proposed scheme, a series of experiments are performed on the UR5 robot and a six-dimensional force/torque sensor HEX-70-X-200N. The maximum load mass of the robot is 5 kg, and the accuracy of the robot is ± 0.1 mm. The 2D vision sensor in our experiments is USBFHD01M. In our experiments, the HEX-70-X-200N F/T sensor is mounted between the peg and the robot end-effector and the charging port is fixed to the shock table as shown in Fig. 1(c).

The overall structure of the experimental platform is as shown in the Fig. 4. The robot is controlled by a computer with Inter(R) i5-3470 CPU with 3.4 GHz speed and 8 GB RAM under a ubuntu16.04 environment. The communication between the robot and the computer is through the Transmission Control Control Protocol/Internet Protocol (TCP/IP).

In the current experiments, it is assumed that the tilt angle of the cover is known. We placed the end in different initial positions, but ensure that the label is included in the end camera view at each initial position. We conducted 50 experiments and succeeded 46 times. In the failed experiments, because the deformation caused by the end of the robot arm was too large, the robot arm failed to open the cover so that the subsequent operations could not be performed. In addition, our method has not yet set the end pose adjustment strategy. Starting from different actual positions, the range of variation of the force/torque data will be offset, but the range of the force/torque data is basically the same. During the course of a successful plug-in-hole experiment, the output values of the force/torque sensor is recorded as shown in Fig. 12. As shown in Fig. 13, we also collected the force/torque data of the manual plug-in-hole operation. After comparison, it can be proved that the real-time values of the Fx, Fy, Fz, Mx, My and Fz in the process of robotic plug-in-hole operation are within a reasonable range, which verified the feasibility of our proposed scheme.

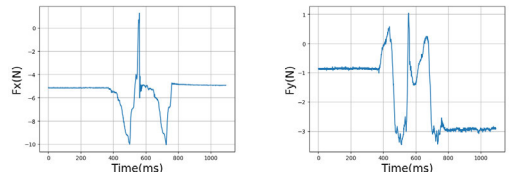

(a) Fx(N)

(b) Fy(N)

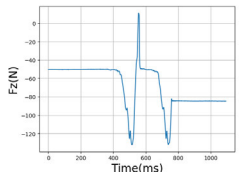

(c) Fz(N)

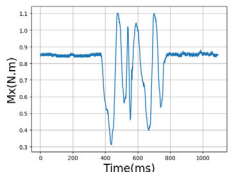

(d) Mx(N.m)

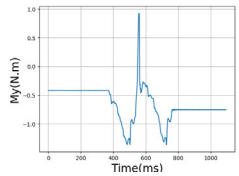

(e) My(N.m)

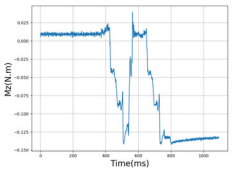

(f) Mz(N.m)

Fig. 12. Force/Torque data curve during robotic plug-in-hole operation

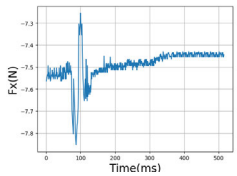

(a) Fx(N)

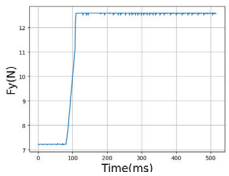

(b) Fy(N)

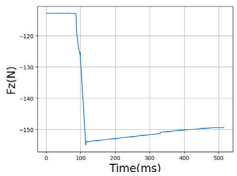

(c) Fz(N)

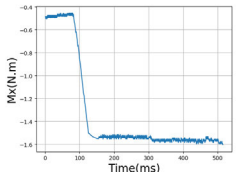

(d) Mx(N.m)

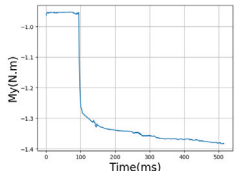

(e) My(N.m)

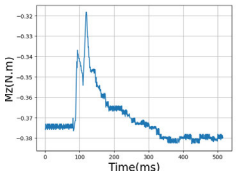

(f) Mz(N.m)

Fig. 13. Force/Torque data curve during manual plug-in-hole operation

V. Conclusions and Future Work

Our method has been proven to be reasonable in the laboratory scenario. In this paper, we abstract the process of the robotic charging of electric vehicles into the cover opening operation and the plug-in-hole operation. The feature-based matching method is used to detect the tag on the charging port. The hand-eye calibration method is applied to obtain the relative position of the camera and the PnP algorithm is used to locate the charging port. The robot arm with the plug at the end goes through the L-shaped path to complete the cover opening operation. Moreover, we design a plug-in-hole control strategy based on the SVM algorithm. Our approach has proved effective in a series of experiments, which will provide theoretical and experimental basis for the practical application of the robotic charging technology in the future.

In the future work, we will try to improve the design of the end connection mechanism, and we will strive to improve the adaptability of our scheme. In addition, we plan to place the robotic arm on the mobile platform and then complete the entire operation.

References

[1] B. Walzel, C. Sturm, J. Fabian, and M. Hirz, "Automated robot-based charging system for electric vehicles," International Stuttgart Symposium. Springer, Wiesbaden, 2016, pp. 937-949.

[2] H. Song, Y. Kim and J. Song, "Automated guidance of peg-in-hole assembly tasks for complex-shaped parts," 2014 IEEE/RSJ International Conference on Intelligent Robots and Systems, Chicago, IL, 2014, pp. 4517-4522.

[3] J. Miura and K. Ikeuchi, "Task-oriented generation of visual sensing stategies in assembly tasks," IEEE Transactions on Pattern Analysis and Machine Intelligence, vol. 20, no. 20, no. 2, pp. 126-138, 1998.

[4] R. Chang, C. Lin and P. Lin, "Visual-based automation of peg-in-hole microassembly process," Journal of Manufacturing Science and Engineering, vol. 133, no. 4, p. 041015, 2011.

[5] S. Huang, and Y. Yamakawa, "Realizing peg-and-hole alignment with one eye-in-hand high-speed camera," in Advanced Intelligent Mechatronics(AIM), 2013 IEEE/ASME International Conference on. IEEE, 2013, pp. 1127-1132.

[6] F. Dakka, and B. Nemec, "Solving peg-in-hole tasks by human demonstration and exception strategies," Industrial Robot: An International Journal 41.6, 2014, pp. 575-584.

[7] T. Inoue, G. Magistris, A. Munawar, T. Yokoya, and R. Tachibana, "Deep reinforment learning for high precision assembly tasks," in 2017 IEEE/RSJ International Conference on Intelligent Robots and Systems (IROS), Sep. 2017, pp. 819-825.

[8] Y. Wang, and P. Wang, "Contact Force/Torque Prediction and Analysis Model for Large Length-diameter Ratio Peg-in-hole Assembly," IEEE International Conference on Robotics and Biomimetics. IEEE, 2018.

[9] Z. Jakovljevic, B. Petrovic, and J. Hodolic, "Contact states recognition in robotic part mating based on support vector machines," The International Journal of Advanced Manufacturing Technology, vol. 59, no. 1-4, pp. 377-395, 2012

[10] H. Bay, T. Tuytelaars, and L. Gool, "SURF: Speeded Up Robust Features," Computer Vision-ECCV 2006, 9th European Conference on Computer Vision, May, 2006.

[11] V. Lepetit, F. Noguer, and P. Fua, "EPnP: An AccurateO(n) Solution to the PnP Problem," International Journal of Computer Vision, 2009, pp. 155-166.

[12] J. Hesch and S. Roumeliotis, "A Direct Least-Squares (DLS) method for PnP," 2011 International Conference on Computer Vision, Barcelona, 2011, pp. 383-390.

[13] R. Tsai and R. Lenz, "A new technique for fully autonomous and efficient 3D robotics hand/eye calibration," in IEEE Transactions on Robotics and Automation, vol. 5, no. 3, June 1989, pp. 345-358.